Journal of Geophysical Research: Biogeosciences

RESEARCH ARTICLE
10.1029/2018JG004690

Production and Transformation of Dissolved and Particulate Organic Matter as Indicated by Amino Acids in the Pearl River Estuary, China

Xiaolin Li[1], Zhanfei Liu[2], Wei Chen[1], Lei Wang[1,3], Biyan He[4], Kai Wu[1], Shuai Gu[1], Peng Jiang[1], Bangqin Huang[1], and Minhan Dai[1]

[1]State Key Laboratory of Marine Environmental Science, Xiamen University, Xiamen, China, [2]Marine Science Institute, University of Texas at Austin, Austin, TX, USA, [3]State Oceanic Administration, Third Institute of Oceanography, Xiamen, China, [4]College of Food and Biological Engineering, Jimei University, Xiamen, China

Abstract Production and transformation of dissolved and particulate organic matter (DOM, POM) in estuaries regulate the carbon export from land to ocean, yet tracing their source and diagenetic status is challenging in these dynamic environments. Here we study the production, transport, and diagenetic status of DOM in the Pearl River Estuary (PRE), China, based on total dissolved amino acids, their enantiomers (D/L ratios), and other ancillary biogeochemical parameters with a complete coverage of upper, middle, and lower estuary. Inferred from amino acid composition and D/L ratios, DOM in the upper PRE was highly altered by bacteria, while the carbon yields of total dissolved amino acids were relatively high showing a conflicting pattern likely contributed by multiple sources including planktonic production, soil leachates, and sewage discharge. Conservative mixing between freshwater and seawater predominantly controlled DOM dynamics in the middle PRE. In contrast, the lower PRE was characterized by high planktonic production, leading to the accumulation of labile DOC in the surface water. The compositional pattern of amino acids differed significantly between dissolved and particulate phases, yet the diagenetic indices of POM and DOM were both relatively lower in the upper and middle PRE compared to the lower PRE, suggesting that primary production is a major driving factor in the lower PRE. Overall, our study emphasizes the highly dynamic and spatially heterogeneous nature of the PRE, and the results from molecular level characterization provide new insights into the complex sources, diagenesis, and transformation processes of DOM in different regions of the estuary, as well as its connection with POM.

Key Points:
- Amino acids and their enantiomers were applied as tracers for diagenetic status of organic materials in the Pearl River Estuary
- Diagenetic status of DOM was regulated by the extent of bacterial alteration, mixing, and primary production in the estuary
- The covaried diagenetic indices of DOM and POM implied that the two organic pools were somewhat coupled in the Pearl River Estuary

Supporting Information:
- Supporting Information S1

Correspondence to:
X. Li,
xlli@xmu.edu.cn

Citation:
Li, X., Liu, Z., Chen, W., Wang, L., He, B., Wu, K., et al. (2018). Production and transformation of dissolved and particulate organic matter as indicated by amino acids in the Pearl River Estuary, China. *Journal of Geophysical Research: Biogeosciences*, *123*. https://doi.org/10.1029/2018JG004690

Received 10 JUL 2018
Accepted 28 OCT 2018
Accepted article online 20 NOV 2018

Author Contributions:
Conceptualization: Xiaolin Li, Zhanfei Liu
Data curation: Lei Wang
Formal analysis: Wei Chen
Investigation: Wei Chen, Shuai Gu, Peng Jiang
Methodology: Xiaolin Li, Lei Wang, Kai Wu
Resources: Biyan He, Bangqin Huang
Supervision: Xiaolin Li
Validation: Xiaolin Li
Writing - original draft: Xiaolin Li
Writing – review & editing: Zhanfei Liu, Biyan He, Bangqin Huang, Minhan Dai

1. Introduction

Estuaries modulate the carbon flux between land and ocean, which is regulated by the physical and biogeochemical processes therein (Bauer et al., 2013). As a major component of the coastal carbon cycle, estuarine dissolved organic matter (DOM) is derived mainly from terrestrial and marine sources, together with in situ production, and often experiences significant removal and transformation during transit due to the combined influences of microbial activity, photooxidation, and sorption to minerals (Hedges & Keil, 1999; Keil et al., 1997; Moran et al., 2000; Smith & Benner, 2005). Even though estuaries have been extensively studied (Benner & Opsahl, 2001; Bianchi et al., 2014; Del Giorgio & Pace, 2008; He et al., 2010), there is uncertainty regarding the major processes that control the removal/accumulation of DOM in different regions of estuaries. In general, the bulk concentration of dissolved organic carbon (DOC) often follows a conservative mixing behavior in estuary, while the specific DOM properties (e.g., molecular composition, absorbance, and bioavailability) are often very dynamic in different estuaries and in different regions of a given estuary (Benner & Opsahl, 2001; Bianchi et al., 2014; Casas-Ruiz et al., 2017; Del Giorgio & Pace, 2008; He et al., 2010; Shen et al., 2016). Focusing only on freshwater or saline water may potentially miss the important biogeochemical processes in the dynamic and heterogeneous estuary. Therefore, it is critical to have a full spatial coverage of the estuary in order to obtain a complete picture of organic matter production and transformation during the transit from river to ocean.

Terrestrial input, in situ production and microbial processing of both particulate organic matter (POM) and DOM in the estuary, can control the type and amount of organic materials exported downstream to coastal waters. The in situ production of DOM derived from phytoplankton blooms in estuaries and adjacent coastal area is an important process that regulates DOM lability and accumulation (Davis & Benner, 2005; Shen et al.,

2016; Wu et al., 2017). Bacterial activity is another important process that shapes the DOM composition and links the transformation between POM and DOM (Davis & Benner, 2005; Kaiser & Benner, 2008). Photo bleaching affects both POM and DOM in estuaries, such as enhancing the dissolution of particles and breaking down chromophores of organic matter (Mayer et al., 2006). Synchronous studies considering both particulate and dissolved organic phases in estuaries have been rare despite their potentially active connections, for example, sources, compositions, and bacterial alteration status.

Molecular level analysis is key to understanding DOM dynamics in estuaries. Of all the characterizable chemical classes, total dissolved amino acids (TDAA), representing a labile fraction of DOM, contribute a dynamic range of carbon to marine DOC from a very small fraction (<1%) in degraded DOM (Shen et al., 2012), to up to 20% in fresh DOM released from phytoplankton (Davis & Benner, 2007; Ittekkot, 1982). The carbon yield of TDAA to DOC can indicate the degree of bioavailable DOM from productive coastal ecosystems to the deep ocean (Druffel et al., 2017; Shen et al., 2016). Enantiomers of amino acids can also be used to trace bacterial sources and diagenetic status of DOM in the ocean, as the fractions of D-forms, from peptidoglycan remnants of bacterial cell walls and bacterial lipopeptides, tend to increase with degradation (Amon et al., 2001; Makovitzki et al., 2006; Mccarthy et al., 1998). Compositional patterns of individual amino acids, when combined with statistical analysis (e.g., principle components analysis), provide further insight into the likely sources and bacterial alteration status in both DOM and POM in estuarine and oceanic environments (Dauwe et al., 1999; Duan & Bianchi, 2007; Kaiser & Benner, 2009; Lee et al., 2000; Yamashita & Tanoue, 2003). Therefore, analysis of molecular indicators provides direct insights into the source and lability of organic matter (Benner & Opsahl, 2001; Shen et al., 2012; Tang et al., 2017).

In this study, DOM production and transformation was investigated in a typical subtropical river estuary, the Pearl River Estuary (PRE), using amino acids and their enantiomers and other ancillary parameters. PRE is the second largest river in China based on discharge volume, and drains into the South China Sea (SCS). PRE is characterized by significantly different biogeochemical processes from the upper to lower estuary (Cai et al., 2004; Harrison et al., 2008; He et al., 2010), and multiple physical and biochemical processes (e.g., river discharge, physical mixing, microbial activities, nutrients supply, and stoichiometry) control the sources, production, and recycling of biogenic elements along the river-estuary-ocean continuum of the PRE ecosystem (Harrison et al., 2008). Samples were collected in high spatial resolution from the whole estuary from the upper to the lower PRE regions. Source, in situ production, and bacterial alteration status of the DOM are evaluated in the different regions of PRE together with the potential connections between DOM and POM.

2. Materials and Methods

2.1. Water Sampling

Water samples were collected using 2.5-L Go-Flo samplers from 33 stations along a salinity gradient of three sampling transects (F, A, and P) in the PRE from 6 to 12 July 2015 (Figure 1). According to historical discharge records, the typical wet season in the PRE is from May to August. During the sampling campaign, the total discharge of the Pearl River reached 16,000 m^3/s, which was comparable to the monthly climatology in July. The DOC exported from the PRE to the continental shelf of the SCS was estimated to be approximately 5.3×10^8 g C d^{-1}, which is about 0.1% of global riverine DOC flux (Dai et al., 2012; He et al., 2010). Temperature and salinity profiles were obtained using a SBE 25 conductivity-temperature-depth/pressure unit (Sea-Bird Co.). Temperature, salinity, and nutrient data were reported in the previous study (Lu et al., 2018). Samples for DOC and TDAA analysis were obtained by filtering water samples through precombusted 0.7-μm GF/F filters. All filtered samples, stored in 40-mL precombusted brown glass vials, were frozen immediately at −20 °C until analysis. Water samples for total amino acids (TAA), including TDAA plus particulate hydrolysable amino acids (PHAA), were stored in 40-mL precombusted brown glass vials without filtration and also frozen immediately at −20 °C until analysis. Samples for particulate organic carbon (POC) and δ^{13}C-POC analysis were collected by filtering a known volume (0.2–1 L) of water through 0.7-μm precombusted GF/F filters under gentle vacuum (<100 mm Hg). Filters were washed with a small amount of distilled water (<2 mL) to remove salts and then stored at −20 °C until analysis. Water samples were collected for pigment measurements which were applied as an indicator for the chemotaxonomy of phytoplankton. In general, 4–8 L water samples were filtered through precombusted GF/F filters under gentle vacuum. The filters were wrapped with aluminum foil and then frozen immediately in liquid nitrogen. Samples for nutrient

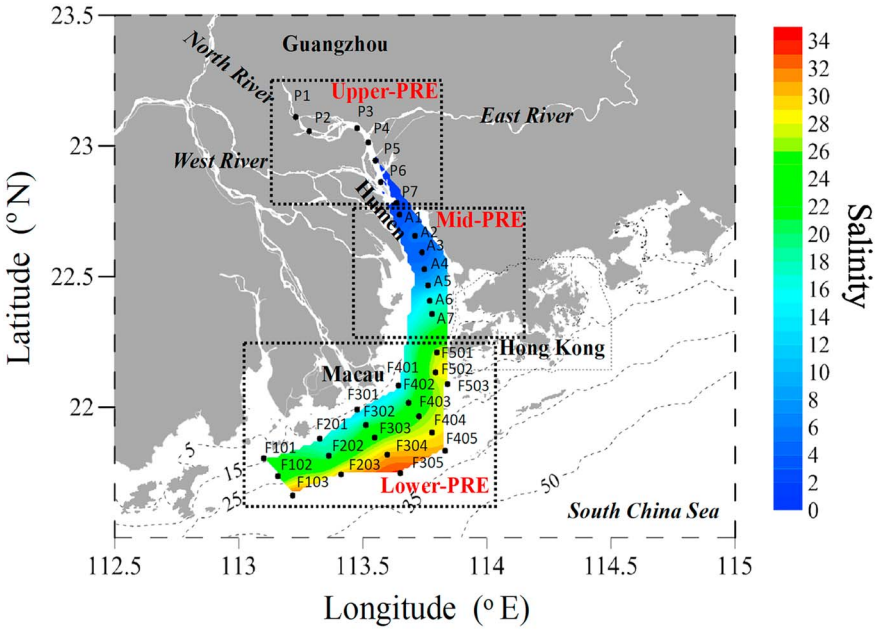

Figure 1. Sampling locations in the Pearl River Estuary (PRE) during the July 2015 cruise. Salinity distributions are shown as a colored contour map, and water depths are shown as dashed contour lines. The research region is divided into the upper, middle, and lower PRE, as shown in the three dashed lined boxes.

analyses were obtained from water filtered through 0.45-μm cellulose acetate filters. Water samples were filtered on preweighed polycarbonate membrane filters for total suspended material determination. Samples used to determine total alkalinity (TA) and dissolved inorganic carbon (DIC) content were collected directly from Go-Flo samplers and placed in separate bottles without air bubbles. The samples for DIC and TA analysis were spiked with 50–100 μL saturated $HgCl_2$ solution to inhibit bacterial activity.

Samples of fresh phytoplankton-released DOM were collected from the culture of *Thalassiosira pseudonana*, a major species of diatom in coastal waters. The culture was grown in sterilized 2-L polycarbonate carboys under continuous light in an algal incubator using filtered (0.22 μm) and microwave-sterilized South China Sea surface water spiked with inorganic nutrients. The samples for DOC and amino acids analysis were gently filtered into the sampling vials through precombusted GF/F filters on the ninth day of culture, at the plateau of the growth phase, and then stored at −20 °C until analysis.

2.2. Chemical Analysis

Details of the pH, DIC, and TA analytical protocols have been described previously (Guo et al., 2009; Zhai et al., 2005). Briefly, DIC and TA analysis had a precision of ±2 μmol/kg. Nutrient samples were stored at −20 °C until analysis except for NH_4^+, which was analyzed on deck using the indophenol blue spectrophotometric method (Pai et al., 2001). Concentrations of NO_2^- and NO_3^- were measured according to colorimetric methods with a Technicon AA3 Auto-Analyzer (Bran-Lube; Han et al., 2012). The detection limits for NO_2^-, NO_3^-, and NH_4^+ were 0.02, 0.07, and 0.16 μmol/L, respectively.

Concentrations of DOC were determined using a TOC analyzer (Shimadzu TOC-V CPH) according to Wu et al. (2015). Briefly, deep seawater (41–44 μmol/L) and low carbon water (1–2 μmol/L), provided by the Hansell Laboratory (University of Miami), were used for quality control on a daily basis during sample analysis. Total blanks associated with DOC analyses were generally about 2–3 μmol C/L, with <2% precision on duplicate analyses. Filters for POC and δ^{13}C-POC analysis were freeze-dried and acidified with 1 mL of 1 N HCl solution to remove carbonates (Casciotti et al., 2008). All filters were then dried at 60 °C for 48 hr in an oven. The decarbonated samples were analyzed for POC and δ^{13}C-POC in a continuous flow elemental analyzer (Carlo-Erba EA 2100) coupled with an isotope ratio mass spectrometer (Thermo Finnigan Delta-plus Advantage), with precision <1% for the standard measurement of δ^{13}C. The δ^{13}C values are reported relative to the Pee Dee Belemnite standard.

Filters for pigment analysis were freeze-dried, soaked in 1 mL N,N-dimethylformamide, and extracted at −20 °C for 2 hr (Furuya et al., 1998). The extracts were passed through GF/F filters to remove particles and then mixed 1:1 with ammonium acetate solution (1 M). A quarter of each mixture was injected into a Shimadzu LC20A-DAD HPLC system fitted with a 3.5-μm C_8 column (100 × 4.6 mm; Agilent Eclipse XDB). Pigment concentrations were quantified with the diode array detector at wavelength of 450 nm following the standard gradient elution procedure (Mendes et al., 2007; Zapata et al., 2000). Quantification was based on authentic standards (Danish Hydraulic Institute Water and Environment, Denmark). The CHEMTAX program was used to derive the community composition of phytoplankton based on the pigment data (Liu et al., 2012).

Analysis of TDAA and TAA was based on an established method (Lindroth & Mopper, 1979). Thirteen amino acids were included in our analysis: aspartic acid (Asp), glutamic acid (Glu), serine (Ser), arginine (Arg), glycine (Gly), threonine (Thr), alanine (Ala), tyrosine (Tyr), valine (Val), phenylalanine (Phe), isoleucine (Ile), leucine (Leu), and γ-aminobutyric acid (GABA). Amino acid calibration standards were purchased from Sigma Chemical. The sampling bottle was vortexed before subsamples of TDAA and TAA were taken. A 2-mL subsample was added to a screw top tube spiked with 2 mL of trace metal clean concentrated HCl (Fisher) and sealed under nitrogen before being hydrolyzed at 110 °C for 24 hr. The hydrolyzed sample was dried with ultrapure nitrogen gas, dissolved in pure water, and then spiked with aminoadipic acid, which served as an internal standard. One milliliter of sample was transferred to a 2-mL vial and then reacted with 100 μL of o-phthaldialdehyde (OPA) solution at room temperature for 2 min. A 20-μL aliquot of the sample was injected into an HPLC system coupled with a fluorescence detector (Shimadzu RF-20A) with excitation and emission wavelengths of 330 and 418 nm, respectively. Separation of amino acids was accomplished using a reverse phase C_{18} column (Inert Sustain, 250 × 4.6 mm, particle size 5 μm) at a flow rate of 1.0 mL/min. Mobile phase A consisted of 0.04 M potassium phosphate monobasic buffer with 1% tetrahydrofuran, and the pH was adjusted to 6.2 with potassium hydroxide. Mobile phase B consisted of HPLC grade methanol, acetonitrile, and ultrapure water mixed at a volume ratio of 4.5:4.5:1. The elution gradient, outlined in Table S1, was performed over 73 min. The relative standard deviation of triplicate analyses was <3%. Concentrations of PHAA were determined by subtracting the TDAA concentrations from the TAA concentrations. Pure water was used as a method blank for every measurement batch. Mean peak areas of each amino acid measured in the blanks were subtracted from the corresponding peaks of all field samples. The method blanks for TDAA and D-AA were generally less than 2% of sample signals measured in this research.

Enantiomeric amino acids were analyzed using the same method as described above but with modified derivative reagents and mobile phases. Briefly, hydrolyzed samples (300 μL) were transferred into 2-mL vials and reacted with 30 μL of OPA-IBL (D) C solution for 2 min at room temperature (Kaiser & Benner, 2005). The derivatized sample (100 μL) was injected into the HPLC system, and the enantiomers were separated with a gradient of organic phase (93% methanol, 7% acetonitrile) and KH_2PO_4 buffer (0.04 M, pH 6.15) as described in Table S2. The flow rate was 0.8 mL/min. The relative standard deviation from triplicate analyses of the enantiomeric amino acid standards was 4%. Four amino acid pairs were included in the analysis: L- and D-aspartic acid, L- and D-glutamic acid, L- and D-serine, and L- and D-alanine. The racemization percentages of the enantiomeric amino acids were lower than 3%, as evaluated by L amino acid standards; thus, the results of D-amino acids were not corrected for racemization.

2.3. Statistical Analysis

The amino acid data were analyzed by principal component analysis (PCA) using R version 3.2.2 (R Development Core Team, 2015) and the package "vegan" (Borcard et al., 2011). In our case the mole percentages of individual amino acids (Table S3) were applied as statistical variables. The optimal weights were created by the principle of least squares, similar to linear regression. The maximum variance in the data is described by the first component, the maximum of the remaining variance by the second, and so forth. Data from different variables were standardized by subtracting the mean value of all samples and divided by the standard deviation.

To evaluate the diagenetic status of organic matter, as indicated by the compositional pattern of amino acids, the degradation index (DI) value was calculated by the following formula (Dauwe et al., 1999):

$$DI = \Sigma_i \left[\frac{var_i - AVG\ var_i}{STD\ var_i} \right] \times fac.coef._i$$

Table 1
Average Concentrations of Dissolved Organic Carbon (DOC), Total Dissolved Amino Acid (TDAA), Diagenetic Index in Dissolved Phase (DI-Dissolved), Particulate Organic Carbon (POC), Particulate Nitrogen (PN), Chlorophyll (Chl), $\delta^{13}C$ of POC, Particulate Hydrolysable Amino Acid (PHAA), and Diagenetic Index in the Particulate Phase (DI-Particle) in the Upper, Middle, and Lower Pearl River Estuary Collected in July 2015

	DOC (μmol/L; n = 98)	TDAA (μmol/L; n = 98)	TDAA Carbon Yield (%; n = 98)	DI-Dissolved (n = 98)	POC (μmol/L; n = 21)	PN (μmol/L; n = 21)	Chl (μg/L; n = 31)	δ^{13}C-POC (‰; n = 21)	PHAA (μmol/L; n = 98)	DI-Particle (n = 98)
Upper PRE	159.2 ± 9.3	1.4 ± 0.5	3.1 ± 1.0	−0.9 ± 0.3	106.3 ± 18.1	14.07 ± 3.44	3.2 ± 2.4	−28.8 ± 0.4	13.5 ± 5.8	−0.07 ± 0.08
Middle PRE	98.2 + 11.0	0.8 ± 0.4	2.5 ± 1.2	−0.8 ± 0.4	29.1 ± 8.0	4.06 ± 1.02	1.6 ± 1.1	−27.9 ± 2.5	2.1 ± 1.9	0.2 ± 0.3
Lower PRE <5 m	98.7 ± 8.0	0.7 ± 0.4	2.6 ± 1.5	−0.2 ± 0.4	54.9 ± 20.3	6.06 ± 2.36	3.8 ± 2.7	−21.0 ± 3.3	3.5 ± 1.7	0.3 ± 0.3
Lower PRE >5 m	82.6 ± 9.2	0.4 ± 0.3	2.1 ± 1.1	−0.2 ± 0.3	-	-	0.7 ± 0.3	-	1.3 ± 0.9	0.2 ± 0.2

where var_i is the mole percentage of amino acid i for particulate or dissolved samples, $AVGvar_i$ and $STDvar_i$ are the mean and standard deviation of the data set, and $fac\text{-}coef._i$ is the factor coefficient for amino acid i which is derived from Table 1 of Dauwe et al. (1999). The DI was originally applied to indicate source and diagenetic status of marine POM, and extended to marine DOM in the later research (Amon et al., 2001; Davis & Benner, 2007). Assuming that organic matter is from the same sources, positive or higher DI values represent labile DOM, whereas negative or lower DI values indicate more degraded DOM.

Significant differences between were tested by independent-sample t test (SPSS 18.0, IBM Statistical Package for the Social Sciences Inc.). The variances of average values are expressed as confidence intervals (p = 0.05).

3. Results

To simplify data presentation and discussion, the study area was divided into three regions (Figure **1**) based on physical locations and biogeochemical processes (Guo et al., 2009; Lin et al., 2016). The upper PRE (stations P1–P7) is located upstream of Humen where freshwater is derived from three major branches, namely, the West, North, and East Rivers (Figure **1**). Middle PRE (stations A1–A7), located between Humen and the barrier islands close to Hong Kong, is the region where freshwater starts to mix with seawater during the wet season. Lower PRE (all F stations) is located at the southwest of the Hong Kong islands and extends to the inner shelf of the northern SCS. Water depths in the upper, middle, and lower PRE are 5–12, 11–16, and 6–36 m, respectively. The salinities in the three regions were 0–3.1, 3.0–31.9, and 13.0–34.5, respectively. The mean values of the selected biogeochemical parameters in the three regions are presented in Table 1. Mixing behaviors and spatial distributions of the biogeochemical and physical parameters in the PRE will be presented on the basis of these three regions.

3.1. Mixing Behaviors of Inorganic and Organic Parameters in the PRE

Inorganic carbon and nutrients were conservatively mixed in the upper and middle PRE during our cruise (Figures 2 and S1). Additionally, TA was conservatively mixed, except for the deviations at salinities <5 (Figure 2a), which may be influenced by input from different Pearl River branches in the upper PRE that exhibit lower alkalinity (Cai et al., 2004; Guo et al., 2008). Conservative mixing of DIC mixing was observed in the middle PRE (Figure 2b); however, this was not the case in the surface samples from the lower PRE, as the values were lower than the conservative mixing curve (red open triangles in Figure 2b). Similar trends were also observed for dissolved inorganic nitrogen (DIN), phosphate, and silicate (Figure S1).

Concentrations of DOC in the upper PRE were in the range of 143.9–176.2 μM, while DOC in the middle and lower PRE ranged from 83.2 to 122.1 and 68.4 to 114.6 μM, respectively (Table 1 and Figure 2c). DOC levels dropped approximately 30% within a small salinity range (0–5) when upstream freshwater began mixing with the seawater, while it was conservatively mixed within the middle PRE region (Figure 2c, blue open squares). Relatively higher levels of DOC were found in the surface water of lower PRE (98.9 ± 8.1 μM; Figure 2c, red open triangles) compared with the middle PRE samples (91.2 ± 6.6 μM, salinity >15) within the same salinity range ($p < 0.0001$).

Compared with DOC, total TDAA concentrations were more variable in the PRE (Figure 2d and Table 1), as indicated by the relatively higher standard deviation of TDAA (63.7%) versus DOC (24.8%). Concentrations of TDAA in the upper PRE (0.78–2.36 μM) were relatively higher than in the middle PRE (0.27–1.69 μM; $p < 0.0001$), while TDAA concentrations in the lower PRE were in the range of 0.15 to 1.84 μM. Generally, TDAA concentrations in the PRE are similar to those in the lower Mississippi River (0.8–2.2 μM; Duan & Bianchi, 2007), and the Louisiana shelf in the northern Gulf of Mexico (0.17–2.08 μM; Shen et al., 2016). Concentrations of TDAA in the surface water from the lower PRE (0.67 ± 0.39 μM) were significantly higher than those from the middle PRE (0.52 ± 0.30 μM, salinity >15) for samples with similar salinities (p = 0.02). The TDAA carbon yield in the upper PRE (~4%) was similar to those in the middle PRE for low-salinity samples, but decreased to <2% in the middle PRE for high-salinity samples. Then, elevated TDAA carbon yields were observed in the surface samples collected from the lower PRE (2.7 ± 1.5%, n = 29; Figure 2e). About half of the surface samples (n = 14) had a TDAA carbon yield >2%, which is in agreement with the observations from the productive "hot spots" on the shelf region in the northern Gulf of Mexico (Shen et al., 2016).

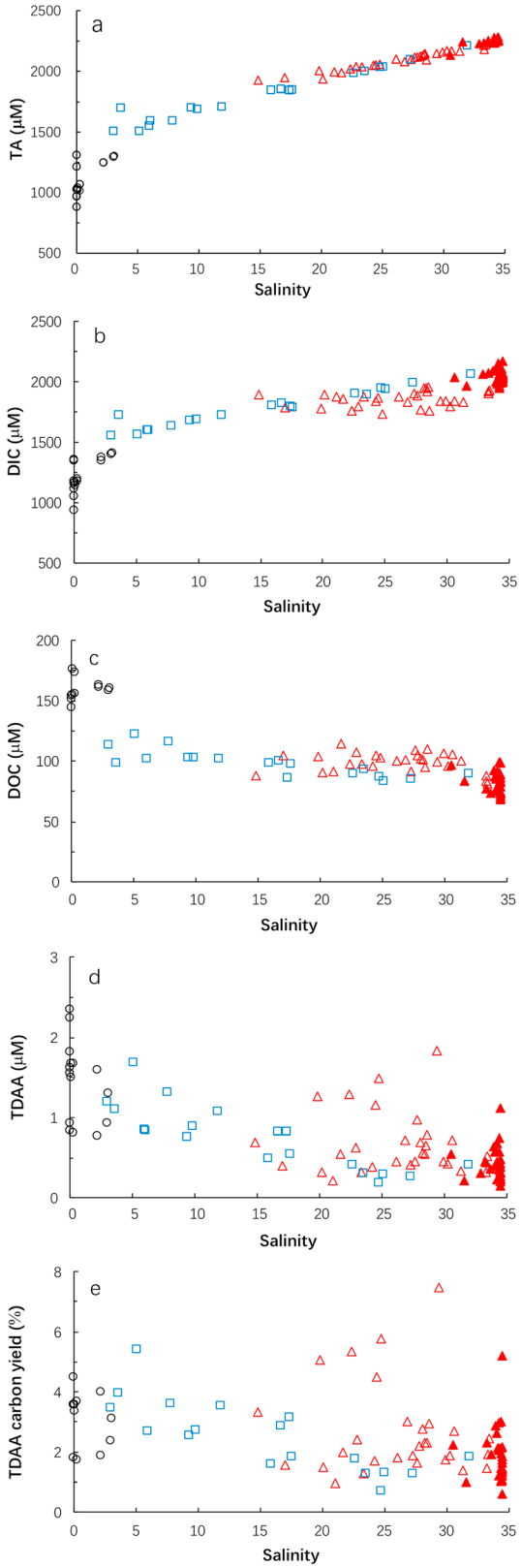

Figure 2. Relationship between (a) total alkalinity (TA), (b) dissolved inorganic carbon (DIC), (c) dissolved organic carbon (DOC), (d) total dissolved amino acid (TDAA), and (e) TDAA carbon yield and salinity in the upper PRE (black empty circles), middle PRE (blue empty squares), lower PRE surface water (red empty triangles), and deeper in the lower PRE (red solid triangles).

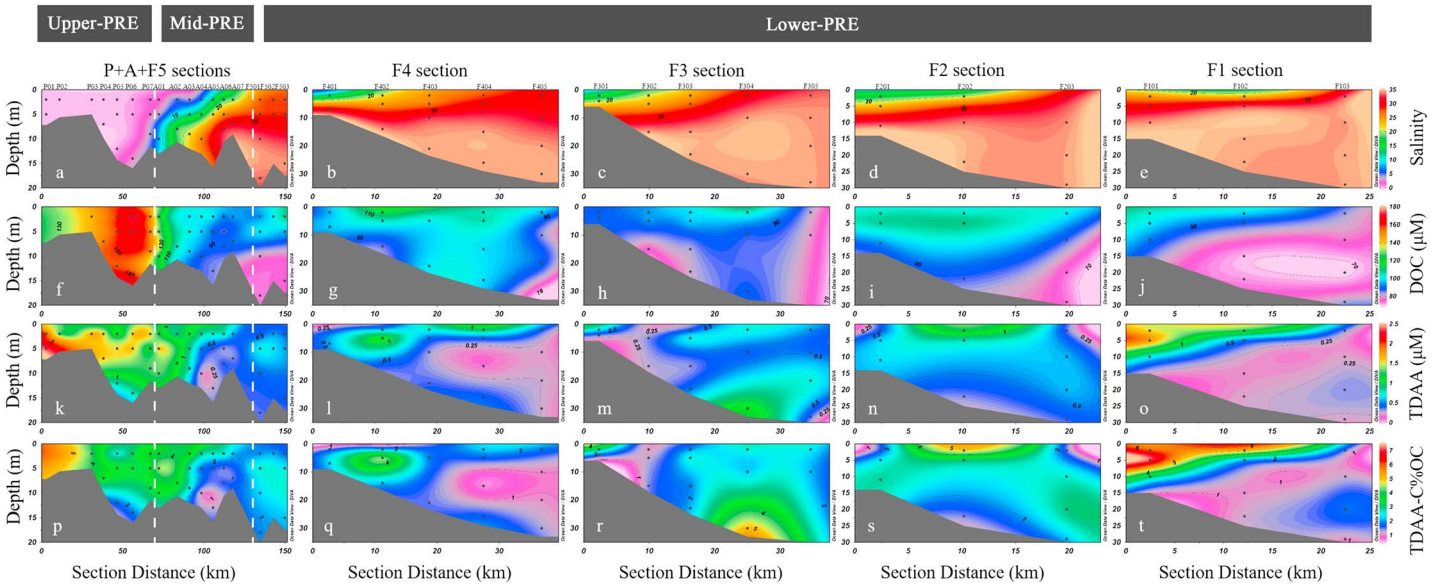

Figure 3. Vertical distribution of (a–e) salinity, (f–j) dissolved organic carbon (DOC), (k–o) total dissolved amino acid (TDAA), and (p–t) TDAA carbon yield along sections P + a + F5, F4, F3, F2, and F1, respectively.

Similar to the dissolved phase, concentrations of POC and Chl *a* were higher in the upper PRE and surface waters of the lower PRE than those in the middle PRE (Table 1 and Figure S2). The δ^{13}C-POC values were gradually enriched from the upper to the lower estuary with values ranging from the upper PRE (−28.6 to −29.1‰) to the lower PRE (−19.8 to −22.6‰). There was no clear correlation between salinity and total suspended material with an average value equaling to 18.3 ± 6.5 mg/L for all samples in the PRE. The highest PHAA concentrations were found in the upper PRE, while the levels decreased with elevated salinity in the middle PRE (Figure S2 and Table S4). Similar to TDAA, higher PHAA levels were found in the surface water samples from the lower PRE samples, relative to the deep lower PRE samples. The phytoplankton community composition, retrieved from accessory pigments, differed significantly between the upper and middle PRE and lower PRE (Figure S3). Diatoms were dominant in the lower PRE, whereas prasinophytes, chlorophytes, and cryptophytes were abundant in the upper and middle PRE.

3.2. Vertical Distribution of Salinity, DO, DOC, TDAA, and TDAA Carbon Yield

The contour maps of salinity showed that freshwater was well mixed in the upper PRE and began to mix with seawater in the middle PRE with clear formation of a salt wedge (Figures 3a–3e). Stratification developed in all the F sections of the lower PRE with a low-salinity surface layer on the top ~5 m. DOC concentrations were relatively higher in the upper PRE and well mixed in the water column (Figure **3**f and Table 1). Despite the salt wedge formation in the middle PRE, DOC levels in the surface water were not significantly different from those in the bottom water (p value = 0.51). In contrast, for the lower PRE, the DOC concentrations were significantly higher in the surface water than those in the deeper water ($p < 0.0001$; Figure **3**). The vertical distribution of TDAA and TDAA carbon yield varied more greatly than DOC in the upper and middle PRE, but exhibited a similar pattern in the lower PRE (Figure **3**). The carbon yields of TDAA in the surface water of the lower PRE (2.7 ± 1.5%, n = 29) were higher than those in the deeper samples (1.9 ± 0.9%, n = 28).

3.3. Compositional Patterns of Dissolved and Particulate Amino Acids

The TDAA compositional patterns in different regions of the PRE are reflected in the PCA results, with principal components (PC) 1 and 2 contributing to 23.8 and 18.1% of the data variance, respectively (Figure 4a). Most of the lower PRE samples are grouped to the right side of the biplot (quadrants I and IV), while most of the middle PRE samples and some of the upper PRE samples are on the left side (quadrants II and III). The separation along the PC1 axis is attributed to mainly six variables, namely, Gly and GABA with negative PC1 values while Phe, Glu, Asp, Ser, and Tyr with positive PC1 values. This pattern shows that the lower PRE samples were enriched with Phe, Glu, Asp, Ser, and Tyr, while the upper and middle PRE samples contained

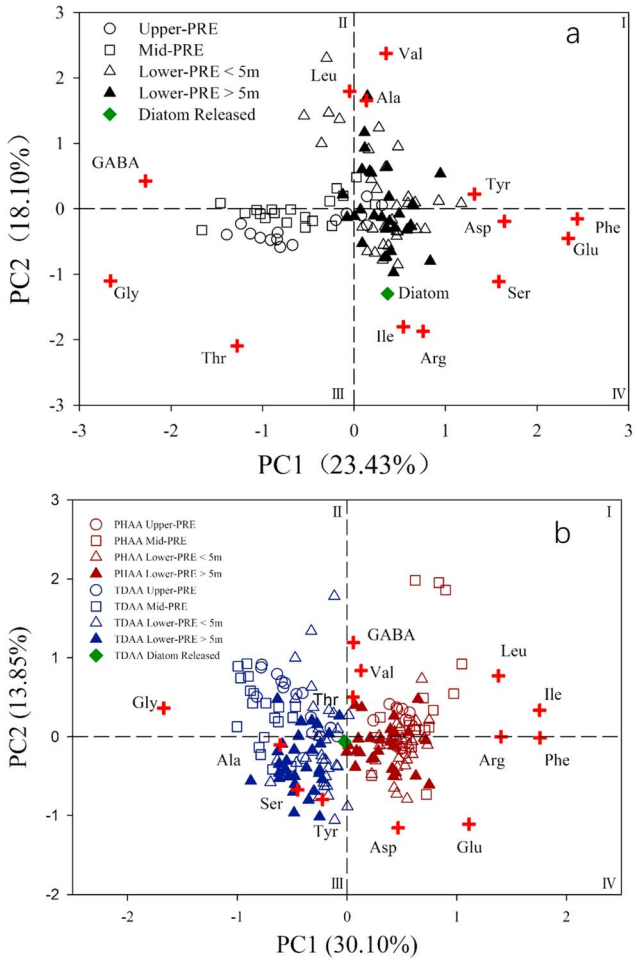

Figure 4. PCA plots of the 13 detected amino acids (red crosses) and (a) all DOM samples and (b) DOM plus POM samples collected from the upper PRE (solid circles), middle PRE (empty squares), and lower PRE surface water and deeper water (empty and solid triangles, respectively) and freshly released DOM from the *Thalassiosira pseudonana* culture experiment (green solid square).

more Gly and GABA. Additionally, the analysis included a fresh DOM sample (TDAA = 3.15 μM, carbon yield = 9.1%) collected from a *T. pseudonana* culture, which is located in quadrant IV, closer to the field samples collected from the lower PRE (Figure 4a). PCA was further performed on both dissolved and particulate samples, with PC1 and PC2 contributing to 30.1 and 13.9% of the data variance, respectively (Figure 4b). The samples of DOM and POM were clearly separated along PC1, which was mainly composed of Ile, Phe, Arg, and Leu with positive PC1 values and Gly with negative PC1 values. The fresh DOM sample collected from the diatom incubation is close to the origin of the coordinates (Figure 4b).

To quantify the diagenetic status of organic matter in the PRE, PCA was performed with the AA molar percentages of all the samples in this study, along with different end-members (fresh plankton, sinking particles, sedimentary organic matter) adopted from Dauwe et al. (1999). The assumption is that degradation of organic matter, in spite of its different sources, follows a similar transformation pattern. The average DI values of the different end-members, as well as the dissolved and particulate phases from the three PRE regions, are shown in Figure 5 and Table 1. As expected, DI values of fresh organic matter, such as bacteria, plankton, and sediment trap materials, were greater than those of sedimentary organic matter, or are more bioavailable. POM samples of the surface water in the lower PRE (0.34 ± 0.28) had the highest DI values, followed by the middle PRE (0.18 ± 0.33), deeper samples of the lower PRE (0.15 ± 0.22), and upper PRE (−0.08 ± 0.08). The DI values for DOM were generally less than those for POM in the four regions, with relatively lower values in the upper and middle PRE (−0.85 ± 0.28 and −0.82 ± 0.42, respectively) than the deeper (−0.22 ± 0.31) and surface samples (−0.19 ± 0.35) in the lower PRE.

The D/L ratios of four major amino acids (Asp, Ser, Glu, and Ala), which generally contribute to more than half of the total TDAA concentrations, were measured between the upper, middle, and lower PRE (Figure S4). The D/L ratios of Asp, Glu, Ser, and Ala in the lower PRE samples were 0.13 ± 0.02, 0.08 ± 0.02, 0.07 ± 0.04, and 0.25 ± 0.02, respectively, while the ratios in the upper stream samples were 0.18 ± 0.03, 0.11 ± 0.03, 0.09 ± 0.02, and 0.30 ± 0.04, respectively. The D/L ratios of Asp and Glu were significantly lower in the lower PRE than in the upper steam samples ($p < 0.05$).

4. Discussion

4.1. Highly Altered DOM in the Upper PRE

In the upper PRE, higher POC, DOC, PHAA, and TDAA levels were caused mainly by terrigenous input combined with in situ production. Depleted δ^{13}C-POC values (−28.6 to −29.1‰) in the upper PRE indicated sources such as plankton, soil, and vascular plants; however, previous work showed that suspended particles in this region were mostly derived from plankton and soils rather than vascular plants (Zhang et al., 2014). Consistently, the biplot N/C ratios and δ^{13}C-POC values of this research and reported end-members of organic matter sources showed that riverine plankton and soil were the main sources of POM in the upper and middle PRE (Figure S5; Goni et al., 2006; Kendall et al., 2001; Lamb et al. 2006; Yu et al., 2010). The river input of DOC derived from soil is expected to be high during the wet season due to the increased surface runoff. Upstream agricultural and urban land use could further facilitate the export of DOM (Stanley et al., 2012; Wilson & Xenopoulos, 2009). He et al. (2010) estimated that the land-derived DOC accounted for approximately 30% of the DOC pool in the upper PRE during the dry season. In addition to soil, in situ production by plankton greatly contributed to organic matter in this region. High concentrations of TDAA in the upper PRE indicated a significant contribution of freshwater planktonic material (Figure 2), which is supported by the high chlorophyll levels, mainly contributed by green algae and diatoms in this region (Figures S2 and S3).

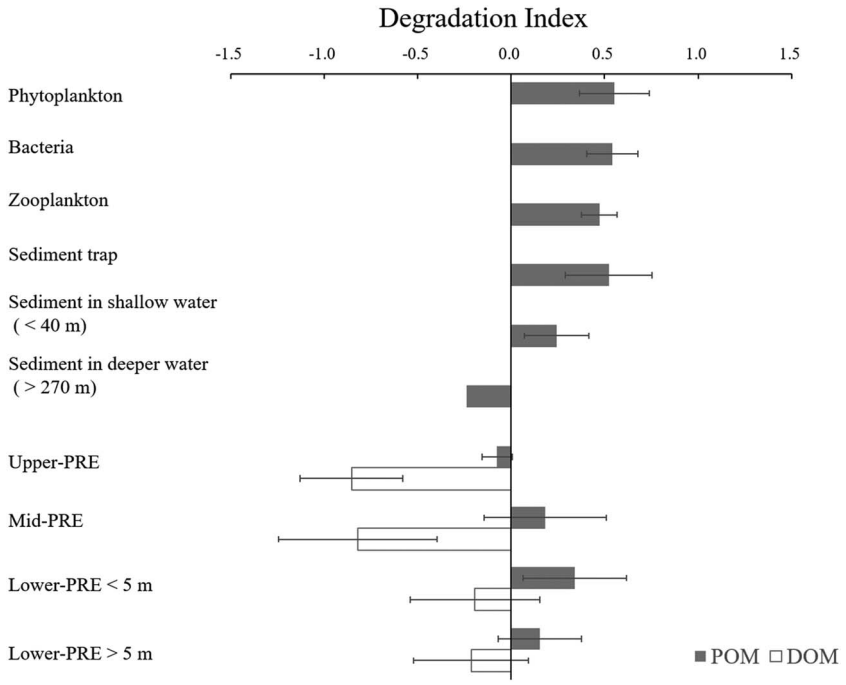

Figure 5. Average diagenetic indexes of phytoplankton (n = 10), bacteria (n = 3), zooplankton (n = 4), and sediment trap POM (n = 27) to sedimentary POM in shallow water (<40-m water depth, n = 5) and the average values of DOM and POM samples collected in the upper, middle, and lower PRE surface and deeper samples. Standard deviations are shown as error bars. Plankton and sediment end-members were adopted from Dauwe et al. (1999), and references therein.

Anthropogenic input of wastewater into the upper PRE is notable due to a high population density and industrial activities in this watershed. For example, up to 8.22×10^9 m^3 of domestic waste and 1.78×10^9 m^3 of industrial effluent were discharged from Guangdong Province in 2015 (Environmental Status Bulletins of Guangdong Province; http://www.gdepb.gov.cn), which is about 2% of the annual discharge of Pearl River. He et al. (2010) observed a high DOC concentration (659 μM) from the sewage effluent near Guangzhou in the upper PRE, which was comparable to the DOC concentration of a field sample (473 μM) collected during the dry season. He et al. further estimated that anthropogenic sources can explain more than half of the DOC found in the upper PRE. During the wet season, the anthropogenic sources of DOC remain important, but may not be as significant as during the dry season due to dilution by the elevated riverine discharge.

Overall, DOM in the upper PRE is a mixture of multiple sources with different stages of diagenetic alteration. As indicated by the compositional pattern of TDAA and the D/L ratios (Figures 4 and S4), DOM in the upper PRE appeared to be bacterially altered. PCA of TDAA compositions showed that Gly, Thr, and GABA were enriched in the DOM of the upper PRE (Figure 4). These amino acids are often accumulated in highly degraded DOM due to the preferential decomposition of labile amino acids (e.g., Glu, Ala) and bacterial production of certain amino acids through enzymatic reactions (e.g., GABA; Amon et al., 2001; Dauwe & Middelburg, 1998; Kaiser & Benner, 2012; Lee & Cronin, 1984). For example, the abundances of Gly, Thr, and GABA in DOM increased during a 10-day incubation experiment using fresh, algal-derived DOM from an Arctic ice floe (Amon et al., 2001). The relatively higher D/L ratios of Asp, Ser, Glu, and Ala (0.18 ± 0.03, 0.11 ± 0.03, 0.09 ± 0.02, and 0.30 ± 0.04, respectively) in the upper stream (salinity <20) provided further evidence that more bacterial alteration of DOM occurred in the upper PRE than in the lower PRE (Figure S4). The D/L ratios of Ser and Ala are within the range observed at the Hawaii Ocean Time Series station (Ser: 0.1–0.5, Ala: 0.3–0.6; Kaiser & Benner, 2008). The decomposition and transformation of organic material in the upper PRE may have been strongly enhanced by in situ bacterial activity (Dai et al., 2006; Guo et al., 2009; He et al., 2010). For example, He et al. (2010) found that the bacterial respiration rate derived from oxygen consumption in the upper PRE was approximately 50 times higher than that in the lower PRE. A significantly higher (>4 times) bacterial abundance has consistently been observed in the upper PRE, compared to the

lower PRE (Zhang et al., 2006; Zhou et al., 2011). The rapid removal of DOC and TDAA in the low-salinity samples (<5; Figure 2) is also consistent with the idea of strong bacterial processing in this region. In addition, DOM from soil and sewage treatment, presumably highly altered, may also contribute greatly to the apparent "degraded" DOM in the upper PRE. Therefore, while the TDAA composition and D/L ratios reflect a highly altered nature of the DOM, the high TDAA carbon yield (~4%) may indicate a significant contribution from primary production considering the high Chl *a* concentrations, further supporting the argument about the multiple sources to the DOM pool in this region.

4.2. Physical Mixing and Transformation of DOM in the Middle PRE

Physical mixing seems to be the dominant biogeochemical process in the middle PRE (salinity >5) based on the conservative behaviors of TA, DIC, DOC, TDAA, and nutrients (Figures 2 and S1). The Chl *a* levels were less than 2 mg/L in most of the middle PRE samples except several samples with high levels at low-salinity stations, which might be influenced by the water from the upper PRE (Figure S2). The low in situ biological production may have been limited by the high turbidity in this region (Cai et al., 2004; Yin et al., 2004). Despite the conservative mixing of TDAA and DOC, the TDAA carbon yield showed that amino acids were preferentially removed (Figures 2e and 2f). There was also a shift in TDAA composition during the mixing process of the middle PRE, as indicated by the PCA (Figure 4a, open squares), with DI values in the range of −1.4 to 0.4. These results suggest that TDAA, as a labile fraction of DOM, can be readily biodegraded within days to weeks (Davis & Benner, 2007; Shen et al., 2016). However, the amount of carbon contributed by TDAA respiration is too small to affect the mixing curves of DOC and DIC (Figure 2). Sorption of natural DOM to minerals could also affect the compositional pattern of amino acids, as basic amino acids are preferentially sorbed to minerals (Aufdenkampe et al., 2001). However, sorption does not seem to be a major process influencing the THAA composition in the PRE. The total suspended material concentration in the PRE was 18.3 ± 6.5 mg/L (Figure S2), which is more than 10 times lower than that in the Amazon estuary (Aufdenkampe et al., 2001). In addition, there were no clear correlations between acidic, basic, hydrophobic, and hydrophilic groups of AAs versus salinity (Figure S6), which further suggests the limited role of sorption in the middle PRE.

4.3. Planktonic Production and Accumulation of Labile DOM in the Lower PRE

Our data suggest that labile DOM accumulates in the surface layer (top 7 m) of the lower PRE because of the elevated primary production. During the wet season, phytoplankton blooms in the lower PRE are triggered by nutrient input from the riverine plume, enhanced stratification, and reduced turbidity in the water column (Dai et al., 2008; Harrison et al., 2008). During our investigation, the water column in the lower PRE was stratified (Figure 3). Significant uptake of DIC in the surface layer clearly indicates high productivity (Figure 2b), which was further confirmed by the higher levels of Chl *a* (dominated by diatom; Figure S3) and POC, as well as marine like δ^{13}C-POC values (−21.0 ± 3.3; Figure S2) and consumption of phosphate and silicate (Figure S1). Diatoms were the dominant phytoplankton species, as indicated by pigment analysis (Figure S3). The higher concentrations of DOC and TDAA, higher TDAA carbon yields, and higher percentages of Glu and Phe (Figures 2 and 4) all indicate that labile DOM was produced and accumulated in this highly productive region. Enrichment of Glu and Phe in the DOM was previously observed during a diatom bloom in the Changjiang River Estuary and its adjacent shelf (Zhang et al., 2015). The composition of TDAA from fresh DOM released by *T. pseudonana*, a common species in coastal waters (Li et al., 2013), is similar to what was found in the DOM of the lower PRE (Figure 4, green diamond).

Net DOM production is often present in coastal oceans due to temporal and spatial uncoupling of biological production and removal (Shen et al., 2016; Wu et al., 2015). Even though it is challenging to estimate DOC accumulation due to complex biochemical and physical processes, a simple two-end-member mixing model can offer a rough estimate of the amount of DOC accumulated and DIC uptake in the surface water of the lower PRE. In this region, the mixing of TA between two selected end-members (F401-surface, salinity = 13; F305-surface, salinity = 33.4) was conservative (Figure 6). The F401-surface sample represented the freshwater end-member jointly influenced by the freshwater discharge from East, North, and West Rivers, the three major branches of the Pearl River. The F305-surface sample represented the surface water of the SCS with a typical salinity for the SCS and a DO saturation equaling to 103%, thereby indicating limited biological impact. This mixing model was also applied to the DOC and DIC mixing models. The biologically modulated DOC and DIC or ΔDOC and ΔDIC were calculated by the following equations:

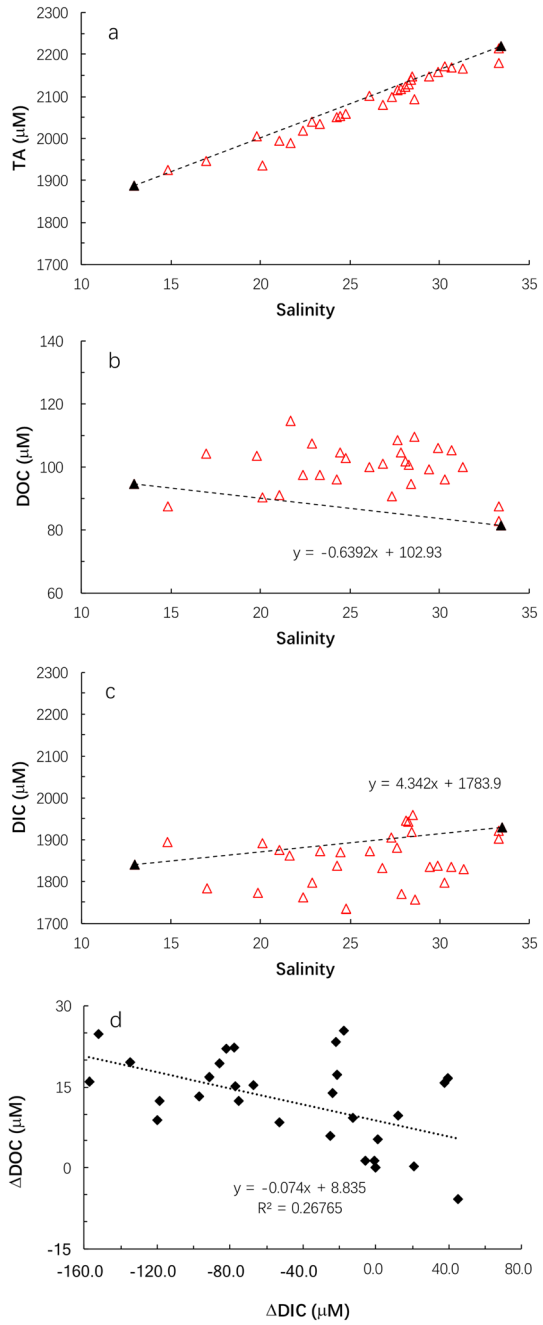

Figure 6. Mixing processes of (a) total alkalinity (TA), (b) dissolved organic carbon (DOC), and (c) dissolved inorganic carbon (DIC) in the surface water of the lower PRE and end-members applied in the mixing model are presented as black solid triangles. (d) Correlations between ΔDOC and ΔDIC are shown with the linear regression plotted (dashed line).

$$\Delta DOC = DOC_{in\ situ} - DOC_{model} \quad (1)$$

$$\Delta DIC = DIC_{in\ situ} - DIC_{model} \quad (2)$$

where $DOC_{in\ situ}$ and $DIC_{in\ situ}$ are the measured DOC and DIC concentrations and DOC_{model} and DIC_{model} are the DOC and DIC concentrations calculated using the conservative mixing model. Most of the surface samples showed accumulation of DOC with positive ΔDOC values (−5.9 to 25.5 μM), while correspondingly, the DIC removal was observed in the region with mostly negative ΔDIC values (−157.2 to −45.2 μM; Figure 6 d). The positive linear correlation between ΔDOC and ΔDIC (r = 0.52, p = 0.003) indicates that, to some extent, the accumulation of DOC is coupled with primary production. For samples in this region, the average ratio of ΔDOC over ΔDIC was approximately 7%, indicating that the fraction of carbon fixed by primary production ended up in DOC. This estimate is consistent with what was estimated in the California current ecosystem, where 11 ± 3% of net primary production was partitioned into total organic carbon which includes DOC and suspended POC (Stephens et al., 2018). However, Wu et al. (2017) reported a higher partitioning ratio (24–26%) in the similar plume region of PRE. Thus, the 7% DOC produced in the PRE plume region is at the lower end of the field observations, which suggests that DOC could be transported across the shelf by coastal currents and eddies (Gan & Qu, 2008). Most of the positive ΔDOC values estimated in the surface water of the lower PRE had phosphate concentrations lower than 0.5 μM when the dissolved inorganic nitrogen was not limiting (average N:P = 177; Figure S7). Liu and Liu (2016) found that a phosphate level of 0.4 μM could limit bacterial degradation of labile DOM (Liu & Liu, 2016). Therefore, the amount of accumulated DOC in coastal regions may be enhanced by reduced microbial activity due to nutrient limitation (Liu & Liu, 2016; Shen et al., 2016; Zweifel et al., 1995).

4.4. Diagenetic Connections of POM and DOM in the PRE

The data set collected in the PRE offers an opportunity to evaluate the diagenetic status of POM and DOM and their transformation in this dynamic estuarine environment. PCA of the AAs in all particulate and dissolved samples from the PRE shows a clear compositional difference between POM and DOM (Figure 4), which could be explained by their different sources and bacterial transformation processes. The enrichment of Phe, Ile, Arg, Leu, Glu, and Asp in PHAA suggests that suspended particles were fresh and sourced from phytoplankton production. In contrast, TDAA contained higher percentages of Gly, Ala, Ser, and Tyr, representing products from bacterial alteration and/or degraded organic matter derived from soil (Amon et al., 2001; Chen et al., 2004; Dauwe et al., 1999; Dauwe & Middelburg, 1998; Lee & Cronin, 1984; Peter et al., 2012). The distinct compositional difference between POM and DOM is expected, as the degree of degradation and age of marine organic matter generally increases with decreasing size (Amon & Benner, 1996; Walker et al., 2016). For example, carbon yield of AAs, as an indicator of lability, decreases with the decreasing size of organic matter from particulate to dissolved phases in the ocean (Benner & Amon, 2015).

Despite the compositional differences of POM and DOM, there is evidence that suggests that they are somewhat coupled. The production of DOM from primary production can be clearly identified in the surface water of the lower PRE using the correlations between DIC removal and DOC accumulation (Figure 6d); for example, DOM and POM are tightly coupled. The fresh DOM from the diatom incubation also resembled the field DOM in this region (Figure 4a). However, this coupling may not be as clear in regions where DOM is derived from

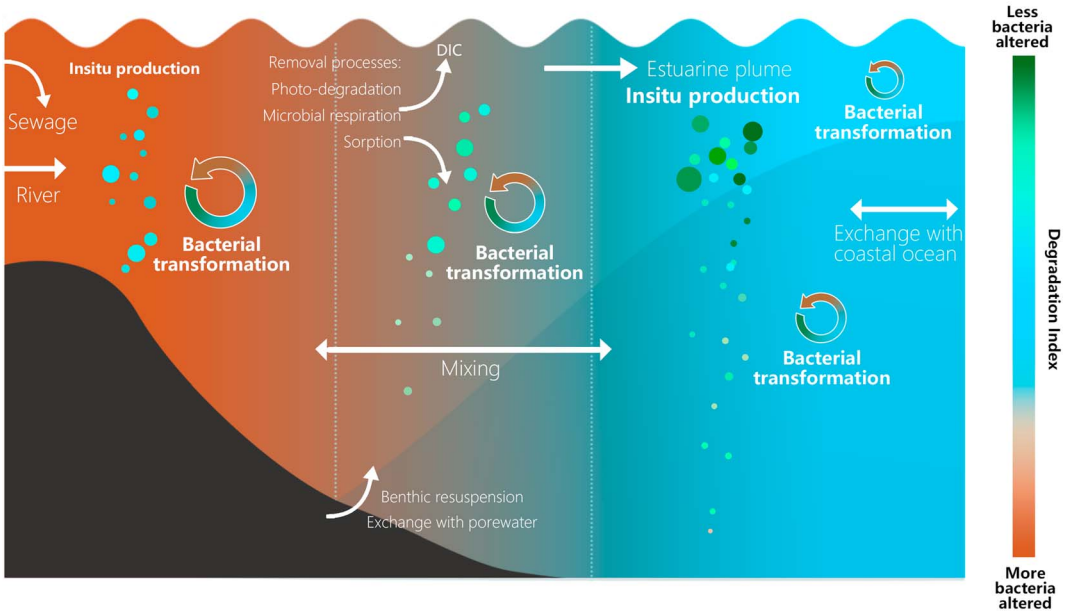

Figure 7. A conceptual diagram showing the diagenetic status of DOM and POM in different regions of PRE during the wet season. The color range of the diagenetic status is referenced from the DI values estimated in this work, and the sources, transport, and transformation processes are shown as arrows in the diagram.

more complex sources and experiences more reworking through bacterial processes; thus, further statistical analysis from molecular composition may be needed in order to gain more insights into the potential coupling. When POM and DOM were inputted into a large data matrix, including end-members (Amon et al., 2001; Dauwe & Middelburg, 1998; Davis & Benner, 2005), they showed a similar shift in diagenetic status from the upper to the lower PRE. The average diagenetic indices of POM and DOM were both relatively lower in the upper and middle PRE, compared to the values in the lower PRE (Figure 5 and Figure S8). These results support the idea that DOM and POM are probably somewhat coupled due to processes that can transform one to the other, such as dissolution, sorption/desorption, aggregation, and disaggregation. For example, photo bleaching can lead to the dissolution of particles into DOM (Mayer et al., 2006; Pisani et al., 2011). However, more direct evidence is needed to demonstrate the coupling of DOM and POM.

5. Summary and Implications

Our results demonstrate that it is critical to have a high spatial resolution sampling of the entire estuary in order to decipher the high spatial heterogeneity of biogeochemical processes. The sources, production, and diagenetic status of DOM were controlled by different processes in the upper, middle, and lower PRE during the wet season, as illustrated in the conceptual diagram (Figure 7). In the upper PRE, DOM is mainly soured from in situ planktonic production, sewage discharge, and soil runoff; a fraction of the DOM was rapidly removed when freshwater mixed with seawater due to strong biological degradation. Bacterial alteration is more intense in the upper and middle PRE than in the lower PRE, as demonstrated by TDAA compositions and relatively higher D/L ratios, as well as the relatively lower DI values in both the POM and DOM. The dynamic processes of organic matter in the upper PRE demonstrate that this estuarine region acts as a reactor rather than a pipe where DOM was decomposed and reworked through intense microbial activities (Casas-Ruiz et al., 2017; Del Giorgio & Pace, 2008). Stratification and riverine input of nutrients favor the planktonic production in the surface water of the lower PRE (Dai et al., 2008; Harrison et al., 2008), thus leading to the accumulation of labile DOM. The mechanisms of labile DOM accumulation need to be further investigated, and as suggested by the previous research, multiple processes, including grazing, phytoplankton excretion, and nutrient limitation of microbial utilization, could synergistically regulate the accumulation (Liu & Liu, 2016; Shen et al., 2016). The compositional pattern of amino acids differed significantly between DOM and POM, owing to their different sources

and extent of microbial transformation, yet they are somewhat coupled. Relying on dense spatial coverage and an enriched data set of biogeochemical parameters, this study highlights the complex production and transformation processes involved in controlling DOM in the upper PRE estuary and offers important insights into DOM dynamics in estuaries before being transported to coastal oceans.

Acknowledgments
This work was supported by the National Natural Science Foundation of China (NSFC; 41676059), the National Key Research and Development Program of China (2016YFA0601203), NSFC (41576085), and the National Key Scientific Research Projects (2015CB954003). This work was also supported by a MEL Senior Visiting Fellowship Award (MELRS1634) and a NOAA grant (NA15NOS4780185) to Zhanfei Liu. Sample collection was conducted onboard R/V "*Kediao 8*." We thank Fengling Yu for her help of sampling and data analysis. We also thank Junhui Chen, Lifang Wang, Zhenyu Sun, Lihua Liu, and Jianzhong Su for their help during sampling and data analysis. We are grateful to Dalin Shi for providing help with the culture experiment. We would like to thank Shuh-Ji Kao and Xianghui Guo for the valuable comments to the manuscript. All data used are listed in the references, tables, and supporting information.

References

Amon, R. M. W., & Benner, R. (1996). Bacterial utilization of different size classes of dissolved organic matter. *Limnology and Oceanography*, *41*(1), 41–51. https://doi.org/10.4319/lo.1996.41.1.0041

Amon, R. M. W., Fitznar, H. P., & Benner, R. (2001). Linkages among the bioreactivity, chemical composition, and diagenetic state of marine dissolved organic matter. *Limnology and Oceanography*, *46*(2), 287–297. https://doi.org/10.4319/lo.2001.46.2.0287

Aufdenkampe, A. K., Hedges, J. I., Richey, J. E., Krusche, A. V., & Llerena, C. A. (2001). Sorptive fractionation of dissolved organic nitrogen and amino acids onto fine sediments within the Amazon Basin. *Limnology and Oceanography*, *46*(8), 1921–1935. https://doi.org/10.4319/lo.2001.46.8.1921

Bauer, J. E., Cai, W. J., Raymond, P. A., Bianchi, T. S., Hopkinson, C. S., & Regnier, P. A. (2013). The changing carbon cycle of the coastal ocean. *Nature*, *504*(7478), 61–70. https://doi.org/10.1038/nature12857

Benner, R., & Amon, R. M. (2015). The size-reactivity continuum of major bioelements in the ocean. *Annual Review of Marine Science*, *7*(1), 185–205. https://doi.org/10.1146/annurev-marine-010213-135126

Benner, R., & Opsahl, S. (2001). Molecular indicators of the sources and transformations of dissolved organic matter in the Mississippi River plume. *Organic Geochemistry*, *32*(4), 597–611. https://doi.org/10.1016/S0146-6380(00)00197-2

Bianchi, T. S., Grace, B. L., Carman, K. R., & Maulana, I. (2014). Amino acid cycling in the Mississippi River plume and effects from the passage of hurricanes Isadore and Lili. *Journal of Marine Systems*, *136*(3), 10–21. https://doi.org/10.1016/j.jmarsys.2014.03.011

Borcard, D., Gillet, F. O., & Legendre, P. (2011). *Numerical Ecology with R*. New York: Springer. https://doi.org/10.1007/978-1-4419-7976-6

Cai, W., Dai, M., Wang, Y., Zhai, W., Huang, T., Chen, S., Zhang, F., et al. (2004). The biogeochemistry of inorganic carbon and nutrients in the Pearl River estuary and the adjacent northern South China Sea. *Continental Shelf Research*, *24*(12), 1301–1319. https://doi.org/10.1016/j.csr.2004.04.005

Casas-Ruiz, J. P., Catalan, N., Gomez-Gener, L., von Schiller, D., Obrador, B., Kothawala, D. N., López, P., et al. (2017). A tale of pipes and reactors: Controls on the in-stream dynamics of dissolved organic matter in rivers. *Limnology and Oceanography*, *62*(S1), S85–S94. https://doi.org/10.1002/lno.10471.

Casciotti, K. L., Trull, T. W., Glover, D. M., & Davies, D. (2008). Constraints on nitrogen cycling at the subtropical North Pacific Station ALOHA from isotopic measurements of nitrate and particulate nitrogen. *Deep Sea Research Part II: Topical Studies in Oceanography*, *55*(14–15), 1661–1672. https://doi.org/10.1016/j.dsr2.2008.04.017

Chen, J., Li, Y., Yin, K., & Jin, H. (2004). Amino acids in the Pearl River estuary and adjacent waters: Origins, transformation and degradation. *Continental Shelf Research*, *24*(16), 1877–1894. https://doi.org/10.1016/j.csr.2004.06.013

Dai, M., Guo, X., Zhai, W., Yuan, L., Wang, B., Wang, L., Cai, P., et al. (2006). Oxygen depletion in the upper reach of the Pearl River estuary during a winter drought. *Marine Chemistry*, *102*(1–2), 159–169. https://doi.org/10.1016/j.marchem.2005.09.020

Dai, M., Yin, Z., Meng, F., Liu, Q., & Cai, W. (2012). Spatial distribution of riverine DOC inputs to the ocean: An updated global synthesis. *Current Opinion in Environmental Sustainability*, *4*(2), 170–178. https://doi.org/10.1016/j.cosust.2012.03.003

Dai, M., Zhai, W., Cai, W., Callahan, J., Huang, B., Shang, S., Huang, T., et al. (2008). Effects of an estuarine plume-associated bloom on the carbonate system in the lower reaches of the Pearl River estuary and the coastal zone of the northern South China Sea. *Continental Shelf Research*, *28*(12), 1416–1423. https://doi.org/10.1016/j.csr.2007.04.018

Dauwe, B., & Middelburg, J. J. (1998). Amino acids and hexosamines as indicators of organic matter degradation state in North Sea sediments. *Limnology and Oceanography*, *43*(5), 782–798. https://doi.org/10.4319/lo.1998.43.5.0782

Dauwe, B., Middelburg, J. J., Herman, P. M. J., & Heip, C. H. R. (1999). Linking diagenetic alteration of amino acids and bulk organic matter reactivity. *Limnology and Oceanography*, *44*(7), 1809–1814. https://doi.org/10.4319/lo.1999.44.7.1809

Davis, J., & Benner, R. (2005). Seasonal trends in the abundance, composition and bioavailability of particulate and dissolved organic matter in the Chukchi/Beaufort Seas and western Canada Basin. *Deep Sea Research Part II: Topical Studies in Oceanography*, *52*(24–26), 3396–3410. https://doi.org/10.1016/j.dsr2.2005.09.006

Davis, J., & Benner, R. (2007). Quantitative estimates of labile and semi-labile dissolved organic carbon in the western Arctic Ocean: A molecular approach. *Limnology and Oceanography*, *52*(6), 2434–2444. https://doi.org/10.4319/lo.2007.52.6.2434

Del Giorgio, P. A., & Pace, M. L. (2008). Relative independence of dissolved organic carbon transport and processing in a large temperate river: The Hudson River as both pipe and reactor. *Limnology and Oceanography*, *53*(1), 185–197. https://doi.org/10.4319/lo.2008.53.1.0185

Druffel, E. R. M., Griffin, S., Glynn, C. S., Benner, R., & Walker, B. D. (2017). Radiocarbon in dissolved organic and inorganic carbon of the Arctic Ocean. *Geophysical Research Letters*, *44*, 2369–2376. https://doi.org/10.1002/2016gl072138

Duan, S., & Bianchi, T. S. (2007). Particulate and dissolved amino acids in the lower Mississippi and Pearl Rivers (USA). *Marine Chemistry*, *107*(2), 214–229. https://doi.org/10.1016/j.marchem.2007.07.003

Furuya, K., Hayashi, M., & Yabushita, Y. (1998). HPLC determination of phytoplankton pigments using N,N-dimethylformamide. *Journal of Oceanography*, *54*(2), 199–203. https://doi.org/10.1007/bf02751695

Gan, J., & Qu, T. (2008). Coastal jet separation and associated flow variability in the southwest South China Sea. *Deep Sea Research Part I: Oceanographic Research Papers*, *55*(1), 1–19. https://doi.org/10.1016/j.dsr.2007.09.008

Goni, M., Monacci, N., Gisewhite, R., Ogston, A., Crokett, J., & Nittrouer, C. (2006). Distribution and sources of particulate organic matter in the water column and sediments of the Fly River Delta, Gulf of Papua (Papua New Guinea). *Estuarine, Coastal and Shelf Science*, *69*(1–2), 225–245. https://doi.org/10.1016/j.ecss.2006.04.012

Guo, X., Cai, W., Zhai, W., Dai, M., Wang, Y., & Chen, B. (2008). Seasonal variations in the inorganic carbon system in the Pearl River (Zhujiang) estuary. *Continental Shelf Research*, *28*(12), 1424–1434. https://doi.org/10.1016/j.csr.2007.07.011

Guo, X., Dai, M., Zhai, W., Cai, W., & Chen, B. (2009). CO_2 flux and seasonal variability in a large subtropical estuarine system, the Pearl River estuary, China. *Journal of Geophysical Research*, *114*, G03013. https://doi.org/10.1029/2008jg000905

Han, A. Q., Dai, M., Kao, S., Gan, J., Li, Q., Wang, L., Zhai, W., et al. (2012). Nutrient dynamics and biological consumption in a large continental shelf system under the influence of both a river plume and coastal upwelling. *Limnology and Oceanography*, *57*(2), 486–502. https://doi.org/10.4319/lo.2012.57.2.0486

Harrison, P. J., Yin, K., Lee, J. H. W., Gan, J., & Liu, H. (2008). Physical–biological coupling in the Pearl River estuary. *Continental Shelf Research*, *28*(12), 1405–1415. https://doi.org/10.1016/j.csr.2007.02.011

He, B., Dai, M., Zhai, W., Wang, L., Wang, K., Chen, J., Lin, J., et al. (2010). Distribution, degradation and dynamics of dissolved organic carbon and its major compound classes in the Pearl River estuary, China. *Marine Chemistry*, *119*(1–4), 52–64. https://doi.org/10.1016/j.marchem.2009.12.006

Hedges, J. I., & Keil, R. G. (1999). Organic geochemical perspectives on estuarine processes: Sorption reactions and consequences. *Marine Chemistry*, *65*(1–2), 55–65. https://doi.org/10.1016/S0304-4203(99)00010-9

Ittekkot, V. (1982). Variations of dissolved organic matter during a plankton bloom: Qualitative aspects based on sugar and amino acid analyses. *Marine Chemistry*, *11*(2), 143–158. https://doi.org/10.1016/0304-4203(82)90038-X

Kaiser, K., & Benner, R. (2005). Hydrolysis-induced racemization of amino acids. *Limnology and Oceanography: Methods*, *3*(8), 318–325. https://doi.org/10.4319/lom.2005.3.318.

Kaiser, K., & Benner, R. (2008). Major bacterial contribution to the ocean reservoir of detrital organic carbon and nitrogen. *Limnology and Oceanography*, *53*(1), 99–1192. https://doi.org/10.4319/lo.2008.53.1.0099, 112.

Kaiser, K., & Benner, R. (2009). Biochemical composition and size distribution of organic matter at the Pacific and Atlantic time-series stations. *Marine Chemistry*, *113*(1-2), 63–77. https://doi.org/10.1016/j.marchem.2008.12.004

Kaiser, K., & Benner, R. (2012). Organic matter transformations in the upper mesopelagic zone of the North Pacific: Chemical composition and linkages to microbial community structure. *Journal of Geophysical Research. Oceans*, *117*, C01023. https://doi.org/10.1029/2011jc007141

Keil, R. G., Mayer, L. M., Quay, P. D., Richey, J. E., & Hedges, J. I. (1997). Loss of organic matter from riverine particles in deltas. *Geochimica et Cosmochimica Acta*, *61*(7), 1507–1511. https://doi.org/10.1016/S0016-7037(97)00044-6

Kendall, C., Silva, S., & Kelly, V. (2001). Carbon and nitrogen isotopic compositions of particulate organic matter in four large river systems across the United States. *Hydrological Processes*, *15*(7), 1301–1346. https://doi.org/10.1002/hyp.216

Lamb, A. L., Wilson, G. P., & Leng, M. J. (2006). A review of coastal palaeoclimate and relative sea-level reconstructions using δ13C and C/N ratios in organic material. *Earth-Science Reviews*, *75*(1–4), 29–57. https://doi.org/10.1016/j.earscirev.2005.10.003

Lee, C., & Cronin, C. (1984). Particulate amino acids in the sea: Effects of primary productivity and biological decomposition. *Journal of Marine Research*, *42*(4), 1075–1097. https://doi.org/10.1357/002224084788520710

Lee, C., Wakeham, S. G., & Hedges, J. I. (2000). Composition and flux of particulate amino acids and chloropigments in equatorial Pacific seawater and sediments. *Deep Sea Research Part I: Oceanographic Research Papers*, *47*(8), 1535–1568. https://doi.org/10.1016/S0967-0637(99)00116-8

Li, Y., Zhao, Q., & Lü, S. (2013). The genus Thalassiosira off the Guangdong coast, South China Sea. *Botanica Marina*, *56*(1). https://doi.org/10.1515/bot-2011-0045

Lin, H., Dai, M., Kao, S., Wang, L., Roberts, E., Yang, J. T., Huang, T., et al. (2016). Spatiotemporal variability of nitrous oxide in a large eutrophic estuarine system: The Pearl River estuary, China. *Marine Chemistry*, *182*, 14–24. https://doi.org/10.1016/j.marchem.2016.03.005

Lindroth, P., & Mopper, K. (1979). High performance liquid chromatographic determination of subpicomole amounts of amino acids by precolumn fluorescence derivatization with o-phthaldialdehyde. *Analytical Chemistry*, *51*(11), 1667–1674. https://doi.org/10.1021/ac50047a019

Liu, X., Huang, B., Liu, Z., Wang, L., Wei, H., Li, C., & Huang, Q. (2012). High-resolution phytoplankton diel variations in the summer stratified Central Yellow Sea. *Journal of Oceanography*, *68*(6), 913–927. https://doi.org/10.1007/s10872-012-0144-6

Liu, Z., & Liu, S. (2016). High phosphate concentrations accelerate bacterial peptide decomposition in hypoxic bottom waters of the northern Gulf of Mexico. *Environmental Science & Technology*, *50*(2), 676–684. https://doi.org/10.1021/acs.est.5b03039

Lu, Z., Gan, J., Dai, M., Liu, H., & Zhao, X. (2018). Joint effects of extrinsic biophysical fluxes and intrinsic hydrodynamics on the formation of hypoxia west off the Pearl River estuary. *Journal of Geophysical Research: Oceans*, *123*, 6241–6259. https://doi.org/10.1029/2018JC014199

Makovitzki, A., Avrahami, D., & Shai, Y. (2006). Ultrashort antibacterial and antifungal lipopeptides. *Proceedings of the National Academy of Sciences of the United States of America*, *103*(43), 15,997–16,002. https://doi.org/10.1073/pnas.0606129103

Mayer, L. M., Schick, L., & Skorko, K. (2006). Photodissolution of particulate organic matter from sediments. *Limnology and Oceanography*, *51*(2), 1064–1071. https://doi.org/10.4319/lo.2006.51.2.1064

Mccarthy, M. D., Hedges, J. I., & Benner, R. (1998). Major bacterial contribution to marine dissolved organic nitrogen. *Science*, *281*(5374), 231–234. https://doi.org/10.1126/science.281.5374.231

Mendes, C. R., Cartaxana, P., & Brotas, V. (2007). HPLC determination of phytoplankton and microphytobenthos pigments: Comparing resolution and sensitivity of a C-18 and a C-8 method. *Limnology and Oceanography: Methods*, *5*(10), 363–370. https://doi.org/10.4319/lom.2007.5.363

Moran, M. A., Sheldon, W. M., & Zepp, R. G. (2000). Carbon loss and optical property changes during long-term photochemical and biological degradation of estuarine dissolved organic matter. *Limnology and Oceanography*, *45*(6), 1254–1264. https://doi.org/10.4319/lo.2000.45.6.1254

Pai, S. C., Tsau, Y. J., & Yang, T. I. (2001). pH and buffering capacity problems involved in the determination of ammonia in saline water using the indophenol blue spectrophotometric method. *Analytica Chimica Acta*, *434*(2), 209–216. https://doi.org/10.1016/S0003-2670(01)00851-0

Peter, S., Shen, Y., Kaiser, K., Benner, R., & Durisch-Kaiser, E. (2012). Bioavailability and diagenetic state of dissolved organic matter in riparian groundwater. *Journal of Geophysical Research*, *117*, G04006. https://doi.org/10.1029/2012jg002072

Pisani, O., Yamashita, Y., & Jaffe, R. (2011). Photo-dissolution of flocculent, detrital material in aquatic environments: Contributions to the dissolved organic matter pool. *Water Research*, *45*(13), 3836–3844. https://doi.org/10.1016/j.watres.2011.04.035

Shen, Y., Fichot, C. G., & Benner, R. (2012). Dissolved organic matter composition and bioavailability reflect ecosystem productivity in the Western Arctic Ocean. *Biogeosciences*, *9*(12), 4993–5005. https://doi.org/10.5194/bg-9-4993-2012

Shen, Y., Fichot, C. G., Liang, S.-K., & Benner, R. (2016). Biological hot spots and the accumulation of marine dissolved organic matter in a highly productive ocean margin. *Limnology and Oceanography*, *61*(4), 1287–1300. https://doi.org/10.1002/lno.10290

Smith, E. M., & Benner, R. (2005). Photochemical transformations of riverine dissolved organic matter: Effects on estuarine bacterial metabolism and nutrient demand. *Aquatic Microbial Ecology*, *40*(1), 37–50. https://doi.org/10.3354/ame040037

Stanley, E. H., Powers, S. M., Lottig, N. R., Buffam, I., & Crawford, J. T. (2012). Contemporary changes in dissolved organic carbon (DOC) in human-dominated rivers: Is there a role for DOC management? *Freshwater Biology*, *57*, 26–42. https://doi.org/10.1111/j.1365-2427.2011.02613.x

Stephens, B. M., Porrachia, M., Dovel, S., Roadman, M., Goericke, R., & Aluwihare, L. I. (2018). Non-sinking organic matter production in the California current. *Global Biogeochemical Cycles*, *32*, 1386–1405. https://doi.org/10.1029/2018GB005930

Tang, T., Filippino, K. C., Liu, Z., Mulholland, M. R., & Lee, C. (2017). Peptide hydrolysis and uptake of peptide hydrolysis products in the James River estuary and lower Chesapeake Bay. *Marine Chemistry*, *197*, 52–63. https://doi.org/10.1016/j.marchem.2017.10.002

Walker, B. D., Beaupré, S. R., Guilderson, T. P., Mccarthy, M. D., & Druffel, E. R. M. (2016). Pacific carbon cycling constrained by organic matter size, age and composition relationships. *Nature Geoscience*, *9*(12), 888–891. https://doi.org/10.1038/ngeo2830

Wilson, H. F., & Xenopoulos, M. A. (2009). Effects of agricultural land use on the composition of fluvial dissolved organic matter. *Nature Geoscience*, *2*(1), 37–41. https://doi.org/10.1038/Ngeo391

Wu, K., Dai, M., Chen, J., Meng, F., Li, X., & Liu, Z. (2015). Dissolved organic carbon in the South China Sea and its exchange with the Western Pacific Ocean. *Deep Sea Research Part II, Topical Studies in Oceanography*, *122*(SI), 41–51. https://doi.org/10.1016/j.dsr2.2015.06.013

Wu, K., Dai, M., Li, X., Meng, F., Chen, J., & Lin, J. (2017). Dynamics and production of dissolved organic carbon in a large continental shelf system under the influence of both river plume and coastal upwelling. *Limnology and Oceanography*, *62*(3), 973–988. https://doi.org/10.1002/lno.10479

Yamashita, Y., & Tanoue, E. (2003). Distribution and alteration of amino acids in bulk DOM along a transect from bay to oceanic waters. *Marine Chemistry*, *82*(3–4), 145–160. https://doi.org/10.1016/s0304-4203(03)00049-5

Yin, K. D., Zhang, J., Qian, P., Jian, W., Huang, L., Chen, J., & Wu, M. C. S. (2004). Effect of wind events on phytoplankton blooms in the Pearl River estuary during summer. *Continental Shelf Research*, *24*(16), 1909–1923. https://doi.org/10.1016/j.csr.2004.06.015

Yu, F., Zong, Y., Lloyd, J., Huang, G., Leng, M., Kendrick, C., Lamb, A. L., et al. (2010). Bulk organic $\delta^{13}C$ and C/N as indicators for sediment sources in the Pearl River delta and estuary, southern China. *Estuarine, Coastal and Shelf Science*, *87*(4), 618–630. https://doi.org/10.1016/j.ecss.2010.02.018

Zapata, M., Rodriguez, F., & Garrido, J. L. (2000). Separation of chlorophylls and carotenoids from marine phytoplankton: A new HPLC method using a reversed phase C-8 column and pyridine-containing mobile phases. *Marine Ecology Progress Series*, *195*(3), 29–45. https://doi.org/10.3354/meps195029

Zhai, W., Dai, M., Cai, W., Wang, Y., & Wang, Z. (2005). High partial pressure of CO_2 and its maintaining mechanism in a subtropical estuary: The Pearl River estuary, China. *Marine Chemistry*, *93*(1), 21–32. https://doi.org/10.1016/j.marchem.2004.07.003

Zhang, G., Liang, S., Shi, X., & Han, X. (2015). Dissolved organic nitrogen bioavailability indicated by amino acids during a diatom to dinoflagellate bloom succession in the Changjiang River estuary and its adjacent shelf. *Marine Chemistry*, *176*, 83–95. https://doi.org/10.1016/j.marchem.2015.08.001

Zhang, Y., Jiao, N. Z., Cottrell, M. T., & Kirchman, D. L. (2006). Contribution of major bacterial groups to bacterial biomass production along a salinity gradient in the South China Sea. *Aquatic Microbial Ecology*, *43*(3), 233–241. https://doi.org/10.3354/ame043233

Zhang, Y. L., Kaiser, K., Li, L., Zhang, D., Ran, Y., & Benner, R. (2014). Sources, distributions, and early diagenesis of sedimentary organic matter in the Pearl River region of the South China Sea. *Marine Chemistry*, *158*(2), 39–48. https://doi.org/10.1016/j.marchem.2013.11.003

Zhou, W., Long, A., Jiang, T., Chen, S., Huang, L., Huang, H., Cai, C., et al. (2011). Bacterioplankton dynamics along the gradient from highly eutrophic Pearl River estuary to oligotrophic northern South China Sea in wet season: Implication for anthropogenic inputs. *Marine Pollution Bulletin*, *62*(4), 726–733. https://doi.org/10.1016/j.marpolbul.2011.01.018

Zweifel, U. L., Wikner, J., Hagstrom, A., Lundberg, E., & Norrman, B. (1995). Dynamics of dissolved organic carbon in a coastal ecosystem. *Limnology and Oceanography*, *40*(2), 299–305. https://doi.org/10.4319/lo.1995.40.2.0299